ELECTRIC RED BEAN PRECISION SEEDING CONTROL SYSTEM BASED ON IHBA-LADRC

/

基于 IHBA-LADRC 的电驱动红豆精量播种控制系统

Yi-fei LI [1,2], Guang-yu WANG [1]; Lin ZHAO [3], Shu-juan YI *[1]
[1] College of Engineering, Heilongjiang Bayi Agricultural University, Daqing, Heilongjiang/ China
[2] College of Engineering, Northeast Agricultural University, Harbin Heilongjiang/ China
[3] College of Basic Education, Beijing Polytechnic University, Beijing/ China
Tel: +86-459-13836961877; E-mile: yishujuan@byau.edu.cn;
Corresponding author: Shu-juan Yi
DOI: https://doi.org/10.35633/inmateh-76-96

Keywords: *red bean, electric precision seeding, control system, IHBA, LADRC*

ABSTRACT

This study proposes an improved honey badger algorithm (IHBA) and a linear active disturbance rejection controller (LADRC) for the electric red bean precision seeder control system to solve high sowing missing rates and uneven sowing in high-density red bean precision sowing. The research details the design process of the intelligent control system, the improvement of the honey badger algorithm, and the intelligent adjustment method for key parameters of the LADRC controller. Simulation experiments show that the IHBA-LADRC based control system has no overshoot, short adjustment time, minimal steady-state error, no oscillation, and strong anti-interference ability. The system achieves an adjustment time of 0.79 seconds, almost zero static error, and an interference recovery time of 0.22 seconds. Bench tests indicate that compared to traditional PID electronic control sowing, the IHBA-LADRC system improves the pass index by 1.32 percentage points, reduces the multiple index by 0.49 percentage points, and lowers the missed sowing index by 0.76 percentage points. The overall variation coefficient decreases by 6.30 percentage points, and the variation coefficient of qualified plant spacing drops by 5.43 percentage points. This system reduces the discrepancy between the actual and theoretical plant spacing of red beans.

摘要

本研究针对高密度红豆精播中的高漏播率和播种不均匀问题，提出了一种改进的蜜獾算法（IHBA）和线性自抗扰控制器（LADRC）用于电动红豆精播机控制系统。该研究详细阐述了智能控制系统的设计、蜜獾算法的改进以及 LADRC 关键参数的智能调整方法。模拟实验表明，基于 IHBA-LADRC 的控制系统具有无超调、调整时间短、稳态误差小、无振荡和抗干扰能力强的特点。该系统实现了 0.79 秒的调整时间，几乎无静态误差和 0.22 秒的干扰恢复时间。台架测试结果表明，与传统的 PID 电子控制播种相比，IHBA-LADRC 系统使格指数整体提高了 1.32 个百分点，重播指数降低了 0.49 个百分点，漏播指数降低了 0.76 个百分点。总体变异系数降低了 6.30 个百分点，合格株距的变异系数降低了 5.43 个百分点。该系统减小了实际株距与理论株距之间的差异。

INTRODUCTION

As an important legume crop, red bean holds a significant place in China's agricultural production. With the advancement of agricultural modernization, red bean seeding technology is continually improving and evolving (*Ma et al, 2022*). To improve the planting efficiency and yield of red beans, electric precision sowing technology ensures that red beans are sown into the soil according to the set spacing, thereby optimizing the allocation of seed resources and increasing crop yield (*Xu et al, 2024*). However, the planting distance of red beans is usually small, and the qualified operational range is narrow, requiring higher control accuracy of the control system. An effective control strategy for the seed discharge motor can improve the performance of the control system (*Li et al ,2024; Ma et al, 2023; Chen et al, 2022*), and many scholars have conducted extensive research in this area (*Wang et al, 2024; Mangus et al, 2017; Ranta et al, 2012*).

Jafari et al. (2010) studied a cereal seeder with variable speed control of a DC motor. The system uses an incremental PID controller to perform closed-loop control. Test results show that the motor can fully adapt to changes in travel speed and reach the set speed in about 6 seconds.

Kamgar et al. (2013) designed an electromechanical transmission system for a conventional row seeder. Their research focused on real-time regulation of the seeding disk's rotation speed through PID control based on speed measurements from a vehicle speed monitoring module. Tests demonstrated that this system can improve the seeding qualification index and reduce missed sowing and variation coefficient. *Cay et al. (2018)* investigated a motor drive system for a single-grain precision seeder. The system comprises an encoder, a brushless DC motor, and its drive module, using pulse width modulation and PID technology for motor control, with a feedback mechanism.

Wang et al. (2022) developed a fuzzy PID control strategy for electric seeding based on GAPSO optimization. GAPSO was used to optimize the two quantization factors, three scaling factors of the fuzzy controller, and the initial values of the three characteristic functions of the PID, leading to improved control system performance. *Ding et al. (2021)* designed a single driver for a corn variable seeder, utilizing the incremental PID algorithm as the control algorithm for the BLDC motor, achieving PID closed-loop control of the seeding motor.

Currently, various electric seeding control methods, both domestically and internationally, mainly use PID control. However, the PID controller has low accuracy and poor anti-interference ability. LADRC can perform real-time feedback compensation for internal and external disturbances in the system. It has the advantage of not relying on an accurate mathematical model of the seeding motor and does not require explicit external interference information for the control system of the electric red bean precision seeder. However, the controller parameter setting is complex, necessitating the introduction of intelligent optimization algorithms. An electric red bean precision seeding control system based on IHBA-LADRC was studied.

MATERIALS AND METHODS

System design

The control system of the electric red bean precision seeder based on IHBA-LADRC mainly consists of the switching power supply, main controller, DC brushless motor, DC motor driver, human-computer interaction interface, air-suction red bean seed metering device, and photoelectric monitoring seed guide tube. The overall structure of the system is shown in Fig. 1.

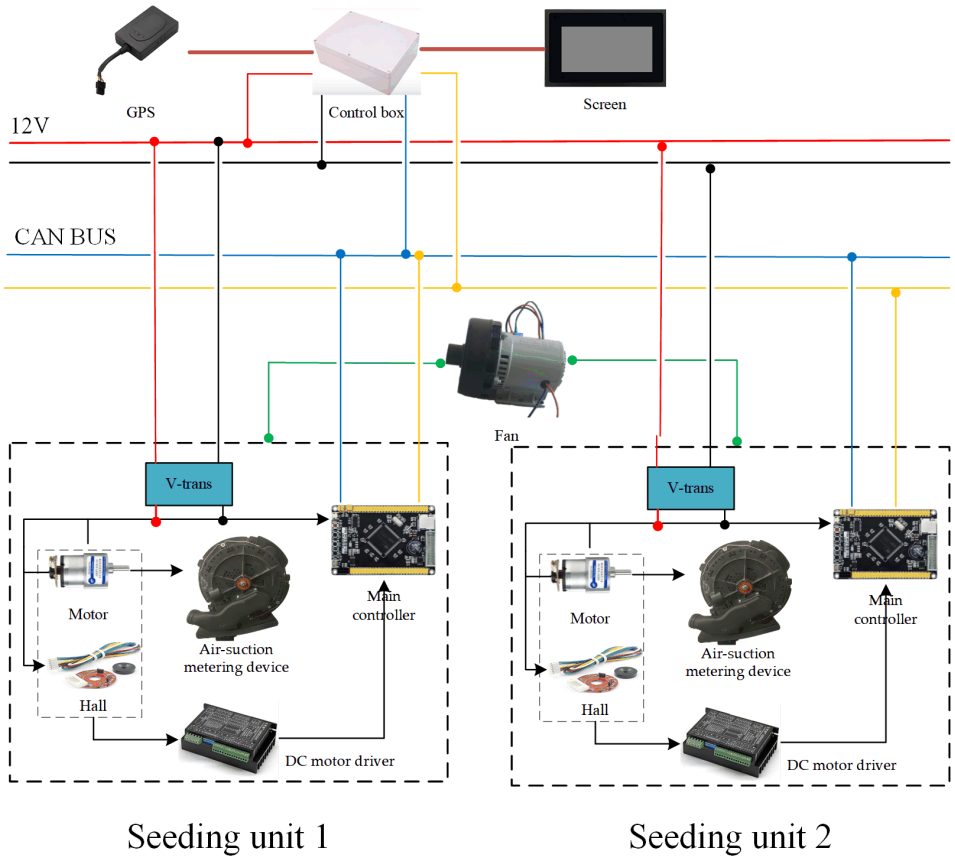

Fig. 1 - Overall system composition diagram

The air-suction red bean seed metering device uses the vSet air-suction seed metering device from Precision Planting Company. The seeding motor is a JGB37-520-CE DC brushless motor produced by ASLONG Company, with a working voltage of 12 V, a no-load speed of 110 r/min, and a rated torque of 0.85Nm. This is greater than the maximum load torque of 0.8 Nm measured by the torque meter when the seed metering device is suctioning, fully meeting the needs of subsequent research. The encoder equipped with the seeding motor is an SCX-Type 520 Hall encoder, a two-channel incremental magnetic encoder suitable for various harsh working conditions, with output in two-way square waves. The main parameters of the seeding motor are shown in Table 1.

Table 1

Motor key parameters of JGB37-520-CE

Motor parameters	Values
Damping coefficient/(N·m·s/rad)	0.0036
Armature resistance/(Ω)	4.3
Armature inductance/(mH)	7.1
Moment of inertia/(kg·cm^2)	220
Rotational acceleration/(rad/s^2)	55

The system's main controller is the STM32F103ZET6 microcontroller, which has 13 communication ports, 144 external pins, integrates 14 timers, and 23 external interrupt controllers, fully meeting current research and future development needs. The human-computer interaction interface uses the DMT10600T070_01W industrial serial screen developed by Beijing Diwen Company, which offers high reliability, good stability, and strong anti-interference ability. The simulated locomotive operating speed and plant distance control seeding motor speed are input through the serial screen. The seeding motor driver uses the MC-FBLD-6600 DC motor driver. The theoretical speed is used as the step input of the closed-loop control, and the speed collected by the encoder serves as the feedback for the closed-loop system, ultimately achieving closed-loop control of the motor speed. The control system circuit of the electric red bean precision seeder is shown in Fig. 2.

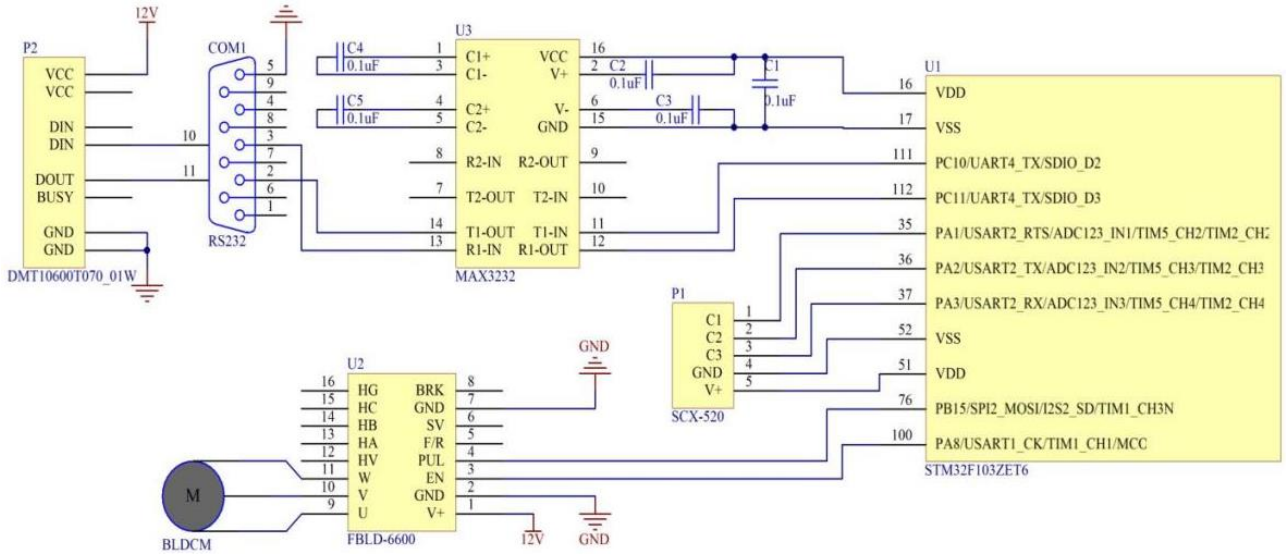

Fig. 2 - Control system circuit of motorized red bean precision planter

Modeling of the seed-rowing motor

To determine the relationship between the motor speed and the operating speed, it is necessary to derive the mathematical relationship between the seeding motor and the machine's traveling speed. The study focuses on an air-suction red bean seed metering device. Assuming there are *m* seed suction holes on the seed plate, the time difference between the dropping of two adjacent red bean seeds is:

$$\Delta t = \frac{60}{nm} \tag{1}$$

where: n is the rotation speed of the seed metering device, r/min.

The formula for calculating the spacing of red bean plants is:

$$Z = 277.78v\Delta t = \frac{1.67\times10^4 v}{nm} \tag{2}$$

where: v is the travel speed of the machine, km/h.

The number of holes in the red bean seed plate of the vSet precision seed metering device selected for the study is 27. Substituting m=27 into the formula (2), the mathematical relationship between the seeding motor and the machine's travel speed can be obtained as:

$$n = \frac{618.52v}{Z} \tag{3}$$

To conduct simulation experiments on the seeding motor control system based on IHBA-LADRC, a physical model of the seeding motor is first established. Compared to the transfer function, the state changes and electrical characteristics of the motor physical model are more similar to the actual seeding motor's changing characteristics and can better simulate the functions and properties of the brushless DC motor (*Zhang et al, 2022; Yousri et al, 2020*). The voltage balance equation of the brushless DC motor is:

$$\begin{bmatrix} U_a \\ U_b \\ U_c \end{bmatrix} = \begin{bmatrix} R & 0 & 0 \\ 0 & R & 0 \\ 0 & 0 & R \end{bmatrix} \begin{bmatrix} i_a \\ i_b \\ i_c \end{bmatrix} + \begin{bmatrix} L-M & 0 & 0 \\ 0 & L-M & 0 \\ 0 & 0 & L-M \end{bmatrix} \begin{bmatrix} \frac{\mathrm{d}i_a}{\mathrm{d}t} \\ \frac{\mathrm{d}i_b}{\mathrm{d}t} \\ \frac{\mathrm{d}i_c}{\mathrm{d}t} \end{bmatrix} + \begin{bmatrix} e_a \\ e_b \\ e_c \end{bmatrix} \tag{4}$$

where:

U_a, U_b, U_c is the phase voltage between windings, *V*; R is the winding phase resistance, Ω; i_a, i_b, i_c is the three-phase phase current, A; L is the stator phase winding self-inductance, H; M is the stator phase winding mutual inductance, H; e_a, e_b, e_c is the three opposite electromotive forces, V.

The expression for the electromagnetic torque of a platoon motor is given by.

$$T_e = \frac{e_a i_a + e_b i_b + e_c i_c}{\omega} \tag{5}$$

where: T_e is the electromagnetic torque, N·m; w is the rotational acceleration, rad/s^2

The rotational acceleration expression is given by:

$$\omega = \frac{2\pi}{60} n' \tag{6}$$

where: n' is the motor rotation speed, r/min

During motor operation, only two of the motor's three-phase windings are active at any moment. Due to the symmetry of the windings, the two active windings have equal amplitude but opposite direction of the reverse electromotive force and phase current. Therefore, it can be derived that:

$$e_a i_a + e_b i_b + e_c i_c = 2E_s I_s \tag{7}$$

$$E_S = \frac{PN}{60}\Phi_m n \tag{8}$$

where:

E_s is the stator voltage, V; I_s is the stator current, A; P is the number of pole pairs of permanent magnets; N is the total number of conductors; Φ_m is the main magnetic flux.

According to Eqs. (6), (7) and (8) the expression for the electromagnetic torque of the platoon motor can be rewritten as.

$$T_e = \frac{2E_s I_s}{\omega} = \frac{PN}{\pi}\Phi_m I_s = C'\Phi_m I_s \tag{9}$$

where: C' is the electromagnetic torque constant

From formula (9), it can be seen that P and N of the seeding motor are constants determined by the motor's inherent properties. The electromagnetic torque T_e of the motor is directly proportional to the main magnetic flux Φ_m and the stator current I_s. Therefore, the motor torque can be adjusted by changing the three-phase stator winding current. The equations of equilibrium of motion of the motor rotor are:

$$T_L = T_e - B\omega + J\frac{\mathrm{d}\omega}{\mathrm{d}t} \tag{10}$$

where:

T_L is the load torque, N·m; B is the damping coefficient, N·m·s/rad; J is the moment of inertia, kg·m^2

When the seeding motor reaches a steady state, the armature windings of any two phases are active, from which the armature circuit voltage loop equation can be derived.

$$U_d = R_s i_a + (L-M)\frac{\mathrm{d}i_a}{\mathrm{d}t} + k_e\omega - \left((L-M)\frac{\mathrm{d}i_b}{\mathrm{d}t} + R_s i_b\right) \tag{11}$$

where: U_d is the bus voltage, V; R_s is the equivalent resistance of each stator winding, Ω

When phases a and b are active, the equivalent resistance and inductance can be established as $R_a=2R_s$ and $L_a=2(L-M)$, because the currents are in opposite directions, $i_p=i_a=-i_b$, so formula (11) can be simplified.

$$U_d = R_a i_p + L_a\frac{\mathrm{d}i_p}{\mathrm{d}t} + k_e\omega \tag{12}$$

The phase voltage of the seeding motor is the input parameter of the control system, and the rotational speed of the seeding motor is the output parameter.

The mathematical model of the seed-rowing motor can be derived as follows.

$$\omega(s) = \frac{K_T U_d(s) - (r_a + L_a s)T_L(s)}{L_a J s^2 + (r_a J + L_a B)s + (r_a B + k_e K_T)} \tag{13}$$

where: K_T is the torque constant of seeding motor.

The equivalent circuit of the brushless DC motor is shown in Fig. 3.

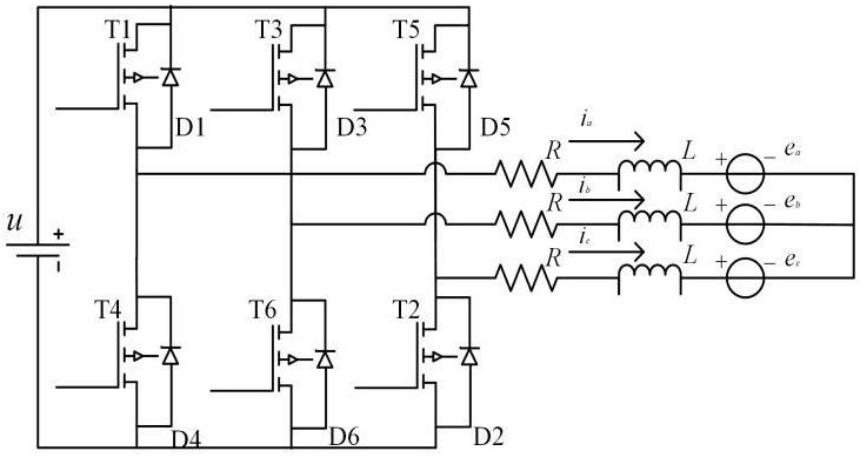

Fig. 3 - Equivalent circuit of the brushless DC motor

Selection of parameters to be optimized by the controller

An active disturbance rejection controller (ADRC) primarily consists of three components: a tracking differentiator (TD), an extended state observer (ESO), and nonlinear state error feedback (NLSEF). Unlike the PID controller, ADRC incorporates the interference signal into the system as a state variable, and then considers interference compensation to minimize the impact of disturbance on the system.

However, ADRC has many components, and there are typically 11 parameters that need adjustment for each component. Manual trial and error is too cumbersome (*Chen, 2008*). Even with optimization algorithms for offline optimization, the complex mathematical model and the number of parameters can lead to excessive computation and long iteration times. Therefore, the literature (*Gao, 2003*) proposes a LADRC, which consists of a TD, a LESO, and a LSEF. LESO is the core control link of LADRC, capable of performing real-time feedback compensation for internal and external disturbances. It does not rely on an accurate mathematical model of the seeding motor, nor does it require clear external interference information for the control system of the electric red bean precision seeder. This greatly reduces the number of parameters that need tuning. Since the DC motor is a second-order system, the expression of the second-order uncertain linear system is:

$$y = f(x_1, x_2, \omega(t)) + bu \tag{14}$$

where: y is the system output; x_1,x_2 is the system parameters; $w(t)$ is the external disturbance; b is the control gain; u is the system input.

The third-order LESO mathematical model can be derived from the second-order linear system state equation:

$$\begin{cases} \dot{z}_1 = z_2 - \beta_1(z_1 - y) \\ \dot{z}_2 = z_3 - \beta_2(z_1 - y) + b_0 u \\ \dot{z}_3 = -\beta_3(z_1 - y) \end{cases} \tag{15}$$

where: β_1, β_2, β_3 is the gain coefficient of LESO,

A PD (proportional-derivative) controller is introduced on the basis of NLSEF to linearize the nonlinear system. Compared with the traditional PD controller, the obtained LSEF reduces the overshoot probability caused by signal mutation. The difference between LSEF and disturbance compensation is:

$$\begin{cases} e_1 = v_0 - z_1 \\ e_2 = -z_2 \\ u_0 = k_p(v_0 - z_1) - k_d z_2 \\ u = (u_0 - z_3)/b \end{cases} \tag{16}$$

where: v_0 is the given value of the controlled object; e_1 is the error input signal; e_2 is the error differential signal; k_p is the proportional coefficient of e_1; k_d is the differential coefficient of e_2.

From equations (8) and (9), it is evident that the performance of the LADRC control system is directly related to the rationalization of the control gain b_0, the gain coefficients β_1, β_2, β_3 of LESO, and the error proportional coefficient k_p and differential coefficient k_d of LSEF. Since there is currently no widely adopted parameter tuning method for LADRC besides the trial and error method, the improved honey badger algorithm is introduced to optimize these six parameters to improve the performance of the control system.

Improving the honey badger algorithm

HBA is a metaheuristic optimization algorithm that simulates the foraging behavior of honey badgers in nature (*Fatma et al, 2021*). Honey badgers are not adept at locating hives, while honey guide birds are not good at opening hives (*Sercan et al, 2023*). HBA is divided into two stages: the excavation stage and the honey collection stage.

The position update formula for the excavation stage is expressed as:

$$x_{new} = x_{prey} + F\beta I x_{prey} + F r_1 w d_i \left|\cos(2\pi r_2)\left[1 - \cos(2\pi r_3)\right]\right| \tag{17}$$

where: x_{prey} is the global optimal position of the prey; $\beta \in [1, \infty)$ represents the honey badger's ability to obtain food, usually set to 6; d_i is the distance between the prey and the i-th honey badger; r_1, r_2, r_3 are three different random numbers in the range of (0,1); I is the odor intensity of the prey, determined by equation (18); w is the update density factor, determined by Eq.(21); F is the sign of changing the search direction, determined by Eq.(22).

$$I = r_4 \frac{S}{4\pi d_i^2} \tag{18}$$

$$S = (x_i - x_{i+1})^2 \tag{19}$$

$$d_i = x_{prey} - x_i \tag{20}$$

$$w = C\exp\left(-\frac{t}{t_{\max}}\right) \tag{21}$$

$$F = \begin{cases} 1, r_5 \le 0.5 \\ -1, \text{else} \end{cases} \tag{22}$$

where: r_4 is a random number within (0,1); S is the source intensity or prey concentration intensity; t_{max} is the maximum number of iterations; C is a constant greater than 1, usually set to 2; and r_5 is a random number within (0,1).

The position update equation for the nectar harvesting phase can be expressed as follows:

$$x_{\text{new}} = x_{\text{prey}} + Fr_6 wd_i \tag{23}$$

where: x_{new} is the new position of the honey badger; x_{prey} is the position of the prey; and r_6 is a random number within (0,1).

The original honey badger algorithm has issues such as slow convergence and a tendency to get trapped in local optima. To address these problems, this paper proposes an IHBA based on a multi-strategy approach. The chaotic mapping algorithm is added in the initialization phase to enable the population to search for the initial operators globally (*Priyadarshi et al, 2023*). Moreover, the human golden ratio segmentation algorithm is added in the variation phase to make the algorithm avoid falling into the local optima (*Anandhakumar et al, 2024*). The density update factor of this algorithm is expressed as:

$$w = 2\left[1 - \sin\left(\left(\frac{t}{t_{\max}}\right)^2 \frac{\pi}{2}\right)\right] \tag{24}$$

The location update equation for the excavation phase is given by

$$x_{\text{new}} = x_{\text{prey}} + F\beta I x_{\text{prey}} + Fr_1 ad_i \left|\cos(2\pi r_2)\left[1 - \cos(2\pi r_3)\right]\right| x_{\text{gnew}} \tag{25}$$

$$x_{\text{gnew}} = x_i \left|\sin(r_7)\right| - r_8 \sin(r_8)\left|c_1 x_b - c_2 x_i\right| \tag{26}$$

$$c_1 = a(1-h) + bh \tag{27}$$

$$c_2 = ah + b(1-h) \tag{28}$$

where: x_{gnew} is the position of the individual after iteration; x_b is the optimal position of the individual; a and b are the initial values of the golden section coefficients, with a=π and b=-π; h is the golden section ratio, approximately 0.6183.

The characteristic parameter process of IHBA optimization of LADRC in Simulink is shown in Fig. 4.

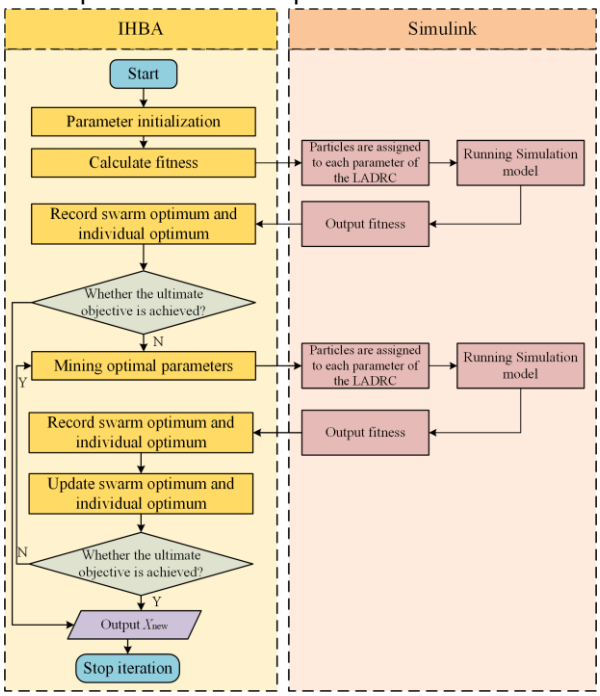

Fig. 4 - IHBA optimization feature parameter process of LADRC in Simulink

IHBA-LADRC controller design

The system objective function used in this study is the ITAE comprehensive evaluation index. This index integrates the product of the running time and the absolute value of the system's steady-state error as the fitness function. A lower ITAE value indicates better control system performance. A control system designed according to this criterion exhibits smaller transient response oscillations and offers good selectivity for parameters. The ITAE calculation formula serves as the fitness function formula:

$$J_{\mathrm{ITAE}} = \int_0^{+\infty} t\left|e(t)\right| \mathrm{d}t \tag{29}$$

where: t is the system running time, s; $e(t)$ is the system steady-state error.

The ITAE index comprehensively evaluates the static and dynamic performance of the control system, including rapidity, accuracy, and stability. This feature helps achieve ideal optimization effects on the steady-state error and adjustment time of the seeding motor.

The input signal should be the expected speed of the seeding motor, calculated by equation (3), and the system control object is the brushless DC motor that drives the red bean precision seeding device. IHBA optimizes the control gain b_0 of LADRC, the gain coefficients β_1, β_2, β_3 of LESO, and the error proportional coefficient k_p and differential coefficient k_d of LSEF. The feedback value of the control system should be the rotor speed of the motor. By comparing the expected speed of the metering device with the actual rotor speed, the speed error e_1 can be obtained. Differentiating this error provides the error change rate e_2. IHBA calculates and evaluates the control system using the ITAE index based on the system error e_1. This process yields the optimal response curve for seeding motor control within the set number of iterations. The IHBA-optimized air-suction electric-driven red bean precision seeder control system LADRC parameter flowchart is shown in Fig.5.

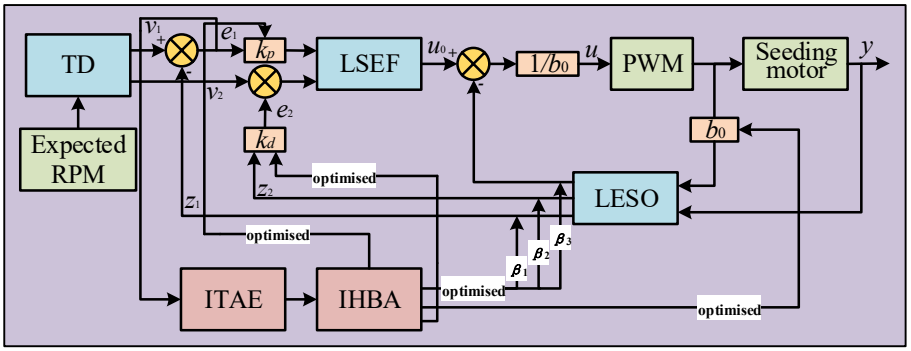

Fig. 5 - IHBA optimized air-suction electric-driven red bean precision seeder system LADRC parameter flowchart

RESULTS

Simulation experiments

The simulation experiment for the electric red bean precision seeder control system, based on the IHBA-LADRC algorithm, uses MATLAB 2022b/Simulink as the test environment. The LADRC-based seeding motor control system is constructed as shown in Fig. 6. Both HBA and IHBA are used to optimize six key LADRC parameters. The experiment compares three seeding motor control strategies: IHBA-LADRC control, empirically tuned PID control, empirically tuned LADRC control, and HBA-LADRC control. This comparison aims to demonstrate the superiority of the IHBA-LADRC-based intelligent control system for the electric red bean precision seeder. In the Simulink simulation, the system running time t is used as the independent variable, the seeding motor speed as the system input, and the unit step response as the output.

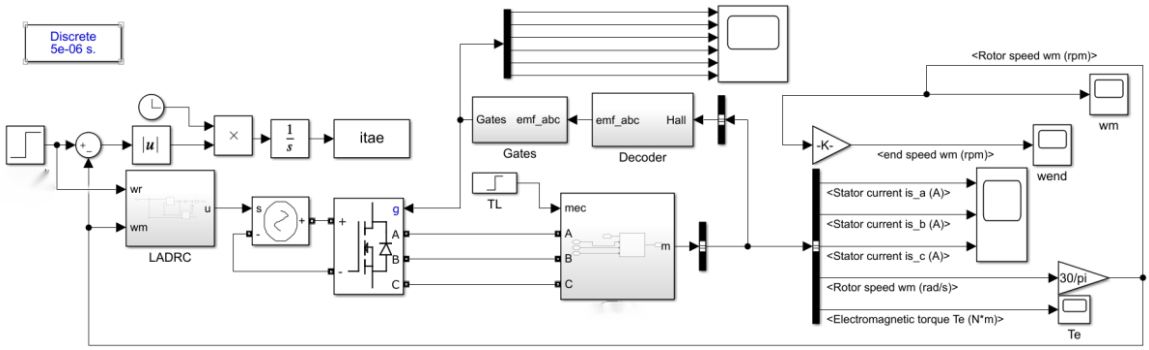

Fig. 6 - Seeding motor control system based on LADRC

Since the simulation experiment involves six optimization parameters, to avoid prolonged simulation times, the optimization scope is narrowed to save time. Before starting the simulation experiment, the six parameters were optimized based on previous empirical adjustments of LADRC parameters. The optimization ranges were set as follows: b_0∈[0.0001,1000], β_1∈[0.0001,1000], β_2∈[0.0001,1000], β_3∈[0.0001,1000], k_p∈[0.0001,1000], k_d∈[0.0001,1000]. The population size for HBA and IHBA is set to 40, and the maximum number of iterations is 100 generations. During sowing operations, various external interferences such as machine tool oscillation and internal interference caused by inconsistent friction factors in different areas inside the seed metering device are common. To evaluate the anti-interference capabilities of the four control strategies, a step disturbance with an intensity of 5 default unit strengths and a disturbance time of 0.2 s was added to the system at 5 s.

The simulation experiments were conducted on an AMD EPYC TM 7642-48C-96T CPU @ 3.0GHz system with 256GB of RAM, running a 64-bit Windows 10 operating system. The simulation software used was MATLAB 2022b/Simulink. Fig. 7 presents the step response curve comparison of the four control strategies, Fig. 7 shows the fitness-iteration number change curve for the two intelligent algorithms, and Table 2 summarizes the control performance indicators for the four control strategies.

Table 2

Comparison of control performance indicators of four control strategies

Control strategies	Overshooting volume δ/%	Adjustment time t_s/s	Steady-state error/ e_{ss}	Interference recovery time t_k/s	Disturbed vibration peak value z/(r·min^{-1})	Adaptation
PID	5.12	0.94	0.012	1.01	45.65	
LADRC	0.37	1.58	0.002	0.45	40.92	
HBA-LADRC	0.02	1.24	0.008	0.20	40.66	3.2036
IHBA-LADRC	0	0.79	0.001	0.22	40.72	1.7611

From Fig. 7 and Table 2, it is evident that the performance indicators of the electric red bean precision seeder control system based on IHBA-LADRC demonstrate significant advantages over the other three control strategies in terms of overshoot, adjustment time, and steady-state error. Specifically, the IHBA-LADRC system exhibits no overshoot, an adjustment time of 0.79 s, almost no static error, a recovery time after interference of 0.22 s, and no oscillation or static error after reaching a steady state again. Although HBA-LADRC and LADRC significantly improve overshoot and steady-state error compared to traditional PID, their anti-interference abilities are not as robust as the IHBA-LADRC. However, there are still certain limitations in optimizing the adjustment time, which remains much greater than that achieved by the IHBA-LADRC algorithm. The anti-interference capabilities of the three LADRCs are significantly better than those of PID. Although the t_k and z values of HBA-LADRC are better than those of IHBA-LADRC, the disturbed vibration peak of IHBA-LADRC is lower. Moreover, there is almost no static difference after it returns to steady state, resulting in better overall stability.

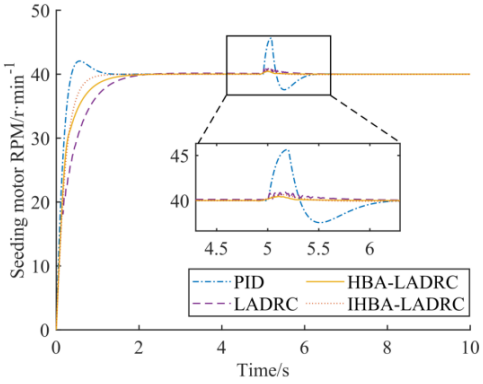

Fig. 7 - Comparison of step response curves of four control strategies

As seen in Fig. 8 and Table 2, the LADRC parameters optimized using IHBA reached the optimal value at the 72nd iteration, with a fitness of 1.7611. In contrast, the LADRC parameters optimized using HBA reached the optimal value at the 85th iteration, with a fitness of 3.2036. IHBA-LADRC demonstrates more iterations and a smaller fitness value, indicating a better control system compared to HBA-LADRC. This validates the improvements made to the HBA in this study.

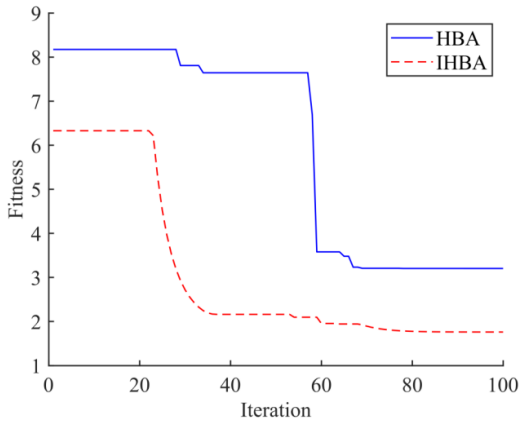

Fig. 8 - Fitness-iterations curve of two intelligent algorithms

Fig. 9 shows the change curves of six key parameters of the LADRC controller optimized by the two intelligent algorithms. As shown in Fig. 9(a), the six parameters of HBA-optimized LADRC are as follows: b_0 reaches the optimal value in the 72nd generation, with an optimal value of 36.7034; k_p reaches the optimal value in the 72nd generation, with an optimal value of 2.3106; k_d reaches the optimal value in the 72nd generation, with an optimal value of 2.8586; β_1 reaches the optimal value in the 72nd generation, with an optimal value of 113.5999; β_2 reaches the optimal value in the 72nd generation, with an optimal value of 387.4995; β_3 reaches the optimal value in the 72nd generation, with the optimal value being 61.2449. As shown in Fig. 9(b),the six parameters of IHBA-optimized LADRC are as follows: b_0 reaches the optimal value in the 85th generation, with an optimal value of 199.3519; k_p reaches the optimal value in the 85th generation, with an optimal value of 17.8458; k_d reaches the optimal value in the 85th generation, with an optimal value of 16.4955; β_1 reaches the optimal value in the 85th generation, with an optimal value of 40.5441; β_2 reaches the optimal value in the 85th generation, with an optimal value of 448.2168; β_3 reaches the optimal value in the 85th generation, with the optimal value being 197.8834.

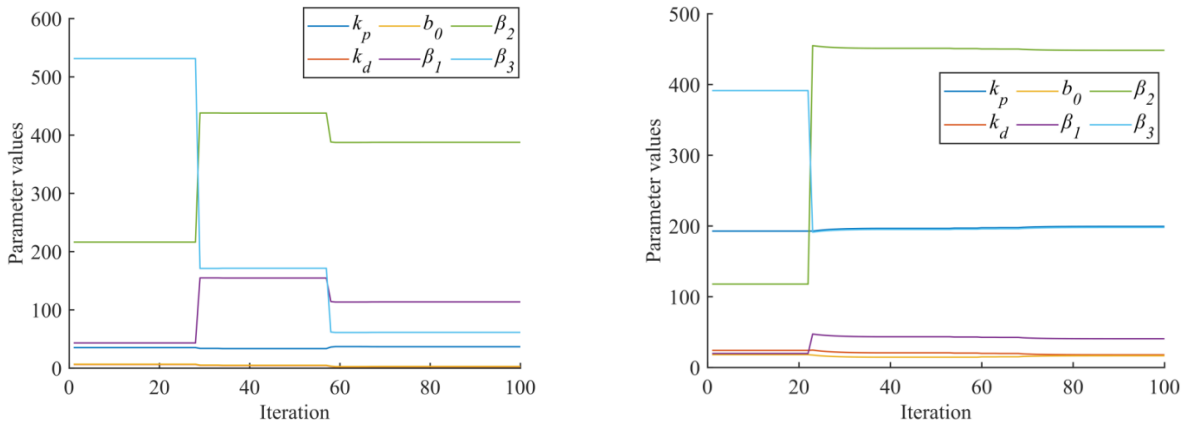

(a) HBA optimized LADRC parameter change curve (b) IHBA optimized LADRC parameter change curve

Fig. 9 - Iterative diagram of two intelligent algorithms optimizing the six key parameters of the LADRC

Seed displacer speed accuracy test

To evaluate the speed accuracy of the control system for the electric air-suction red bean precision seeder, a seed metering speed accuracy test was conducted. The test took place on March 26, 2024, in the High-speed Precision Seeding Laboratory of Heilongjiang Bayi Agricultural University. Using the DT-2234A photoelectric speedometer (accuracy: ±0.1 r/min) developed by the Lutron Company, the actual rotation speed of the seed metering device was collected. This was done when the theoretical plant spacing was 100 mm and the operating speed was set at 3, 5, 7, 9 km/h. The speed of the seeding motor was recorded 30 seconds after stabilizing, and the average speed *N* of the seeding device was calculated. Each set of speeds was repeated 8 times (N1~N8), and the coefficient of variation of the actual speed of the seeding device was determined. Table 3 presents the results of the seed metering speed accuracy verification test.

Table 3

Verification experiment table of speed accuracy of seed metering device

Working speed/(km·h^{-1})	Theoretical speed/(r·min^{-1})	Actual speed/(r·min^{-1})								Average speed/(r·min^{-1})	Coefficient of variation/%
		N_1	N_2	N_3	N_4	N_5	N_6	N_7	N_8		
3	18.6	19.0	18.1	19.5	18.2	19.4	18.3	18.0	19.2	18.7	3.34
5	31.0	30.1	31.8	31.5	30.4	32.2	30.2	31.7	30.3	31.0	2.76
7	43.3	42.6	44.5	42.6	42.7	43.8	42.7	43.2	42.4	43.1	1.61
9	55.7	54.4	57.7	53.9	54.0	53.5	56.8	53.4	58.1	55.2	3.56

As shown in Table 3, the electric red bean precision seeder control system based on IHBA-LADRC shows superior seed metering speed accuracy and uniformity, with seed metering speed variation coefficients of less than 4%. At operating speed of 9 km/h, the coefficient of variation of the actual rotation speed of the seed metering device reaches a maximum of 3.56%. At operating speed of 7 km/h, this coefficient reaches a minimum of 1.61%. When operating at 9 km/h, N_5 shows the maximum speed deviation, with a deviation rate of 4.31%. At 7 km/h, N_5 shows the minimum speed deviation, with a deviation rate of 0.23%.

Seed discharge performance static test

To further verify the superiority of the IHBA-LADRC intelligent control strategy obtained from the simulation experiments, a bench comparison test was conducted. This test compared the performance of the intelligent electric seeding system, the traditional PID electric seeding system, and the sprocket seeding system. The test took place in the High-speed Precision Seeding Laboratory of Heilongjiang Bayi Agricultural University from April 5 to April 7, 2024. The test materials included the red bean hybrid "Jihong No. 7,". This hybrid has a moisture content of (13.1±0.87)%, a thousand-grain weight of (202.2±0.85)g, a density of (1.24±0.06) g·cm^{-3}, and a seed clarity of 97.96%. The seeds are ellipsoid in shape, with a sphericity of 80.1%, and dimensions of (8.09±0.78) mm in length, (5.81±0.40) mm in width, and (5.78±0.40) mm in height. The test was conducted on April 30, 2024, in the Seeding Equipment Laboratory of the Heilongjiang Bayi Agricultural University. The laboratory is equipped with a JPS-12 computer vision seed metering device performance testing device. The seeding performance test setup is shown in Fig. 10.

Fig. 10 - Seeding performance experiment device

Red beans are planted at densities where the distance between plants is determined to be 100~150 mm according to the indicators. After preliminary testing and calibration, it was found that seeds can be planted evenly when the operating speed is below 10 km/h and the wind pressure in the seed suction room is between -1~-1.5 kPa. To minimize variables and reduce the number of test groups in the comparison test, the fan's negative pressure was fixed at -1.5 kPa, and the seeding height was set at 50 mm. Three different groups of sowing at plant spacings of 100 and 150 mm were selected at four different operating speeds of 3, 5, 7, and 9 km/h. These were used to compare the performance of chain-driven and electric-driven red bean precision sowing operations, following GB/T 6973-2005 "Test Method for Single-Seed (Precision) Seeder"(*Yi et al, 2025; Sun et al, 2024; Wang et al, 2024*). The qualified index, multiple index, missing index, and coefficient of variation were used as evaluation indices. Additionally, the coefficient of variation for qualified spacing was introduced to determine the stability of the electric seeding control system designed in this study.

The coefficient of variation for qualified spacing measures the variation in spacing among qualified seeds, excluding reseeding and missed seeding caused by seed arranging device defects and external interference. This metric helps to determine the uniformity of sowing qualified red bean seeds, thereby validating the superiority of the designed control system. Ideal spacing uniformity is crucial for subsequent field management activities such as fertilization and spraying. In each bench test, 30 consecutive spacing samples were selected from the seed bed after the stable operation of the electronic control system. Each test group was repeated three times, resulting in 90 spacing samples for analysis and calculation of operational indexes. The results of the bench test are shown in Table 4.

Table 4

Bench experiment results

Working distance / mm	Operational indicators	Seeding operation speed (chain drive)/(km·h^{-1})				Seeding operation speed (PID electric drive)/(km·h^{1})				Seeding operation speed (intelligent electric drive)/(km·h^{-1})			
		3	5	7	9	3	5	7	9	3	5	7	9
100	Qualified index	92.22	93.33	93.33	90.56	94.45	93.89	95.56	94.45	94.45	96.11	97.22	94.45
	Multiple index	1.11	2.22	2.22	3.33	2.22	2.22	1.11	2.22	2.22	1.11	0.56	2.22
	Missing index	6.67	4.45	4.45	6.11	3.33	3.89	3.33	3.33	3.33	2.78	2.78	3.33
	CV	26.56	27.89	26.96	29.39	23.89	24.00	22.94	26.18	20.21	16.95	13.63	20.05
	CV of spacing	19.91	19.08	18.24	20.73	15.45	15.13	15.95	19.26	9.62	12.13	7.83	12.07
150	Qualified index	94.45	95.56	95.56	93.34	96.11	95.56	95.56	95.00	96.67	97.78	97.78	96.67
	Multiple index	2.22	1.11	1.11	2.22	1.11	2.22	2.22	1.11	1.11	1.11	1.11	1.11
	Missing index	3.33	3.33	3.33	4.44	2.78	2.22	2.22	3.89	2.22	1.11	1.11	2.22
	CV	23.04	21.56	22.73	26.04	20.88	21.59	20.11	22.49	16.84	13.90	12.46	17.67
	CV of spacing	15.87	16.18	17.07	19.39	14.98	13.86	12.53	15.30	9.56	8.46	7.91	11.52

As seen in Table 4, the IHBA-LADRC-based electric red bean precision seeder control system significantly improves various sowing operation indicators compared to the traditional sprocket seeding system and the traditional PID electric seeding system. At four different operating speeds, when the theoretical plant spacing of red beans is 100 mm, the average passing index of the intelligent electric-driven sowing system is 3.20 percentage points higher than that of the sprocket sowing system. The average multiple index is reduced by 0.69 percentage points, and the average missing index is reduced by 2.36 percentage points. Additionally, the average coefficient of variation decreased by 9.99 percentage points, and the average coefficient of variation for qualified plant spacing decreased by 9.08 percentage points. Compared to the traditional PID electric seeding system, the intelligent electric seeding system's average qualified index increased by 0.97 percentage points, the average reseeding index decreased by 0.41 percentage points, and the average missed sowing index decreased by 0.41 percentage points. The average variation coefficient decreased by 6.54 percentage points, and the average variation coefficient for qualified plant spacing decreased by 6.04 percentage points.

When the theoretical plant spacing of red beans is 150 mm, the average qualified index of the intelligent electric seeding system is 2.50 percentage points higher than that of the sprocket seeding system. The average reseeding index is reduced by 0.56 percentage points, the average missed sowing index is reduced by 1.94 percentage points, and the average variation coefficient is reduced by 8.12 percentage points. The average variation coefficient for qualified plant spacing decreased by 7.77 percentage points. Compared to the traditional PID electric-driven sowing system, the average qualified index of the intelligent electric-driven sowing system increased by 1.67 percentage points, the average multiple index decreased by 0.56 percentage points, the average missed sowing index decreased by 1.11 percentage points, the average variation coefficient decreased by 6.05 percentage points, and the average qualified plant spacing variation coefficient decreased by 4.81 percentage points.

The data above demonstrates that compared to the chain-driven seeding system, the intelligent electric seeding system shows an overall improvement of 2.85 percentage points in the qualified index, a reduction of 0.63 percentage points in the multiple index, and a reduction of 2.15 percentage points in the missed seeding index across different plant spacings and operating speeds.

Additionally, the overall coefficient of variation decreased by 9.06 percentage points, and the coefficient of variation for qualified plant spacing decreased by 8.43 percentage points. Compared to the traditional PID electric seeding system, the intelligent electric seeding system exhibits an overall improvement of 1.32 percentage points in the qualified index, a reduction of 0.49 percentage points in the multiple index, and a reduction of 0.76 percentage points in the missed seeding index across different plant spacings and operating speeds. The overall coefficient of variation decreased by 6.30 percentage points, and the coefficient of variation for qualified plant spacing decreased by 5.43 percentage points.

Compared to the sprocket-driven seeding system and the PID electric-driven seeding system, the intelligent electric seeding system significantly reduces the missed seeding rate and coefficient of variation in the red bean seeding process. It also improves the uniformity of the spacing of qualified red bean plants, as evidenced by the significantly reduced variation coefficient of qualified plant spacing. This improvement ensures that the actual planting of red beans is less variable than the theoretical plant spacing, resulting in evenly aligned seeds between ridges and consistent plant numbers. This uniformity facilitates follow-up field management for farmers.

CONCLUSIONS

(1) To address the high sowing missing rate and uneven sowing due to small theoretical plant spacing, narrow qualified range, and internal and external interference during precision sowing of red beans in high-density planting, an electric red bean precision seeder control system based on IHBA-LADRC was studied. The design process of the intelligent control system, the improvement of the honey badger algorithm, and the intelligent tuning method of key parameters in the LADRC controller are explained. This system addresses the issues of long adjustment time, large overshoot, significant steady-state error, and poor anti-interference ability in general electric seeding systems.

(2) The simulation experiment results demonstrate that the control system of the electric red bean precision seeder based on IHBA-LADRC exhibits no overshoot, short adjustment time, minimal steady-state error, no oscillation, and strong anti-interference ability. Among the four algorithms tested, the dynamic response characteristics are optimal. The IHBA algorithm enables the optimal intelligent control strategy in the electric seeder control system. The system reaches steady state with an adjustment time of 0.79 s, shows nearly zero steady-state error, recovers from disturbances within 0.22 s, and maintains stability without oscillations after returning to steady state.

(3) Bench test results show that under four different operating speeds and three different theoretical plant spacings, the electric red bean precision seeder control system based on IHBA-LADRC outperforms the sprocket seeding system in various seeding performance indicators. The overall qualified index increased by 2.85 percentage points, the reseeding index decreased by 0.63 percentage points, the missed seeding index decreased by 2.15 percentage points, the coefficient of variation decreased by 9.06 percentage points, and the variation coefficient of qualified plant spacing decreased by 8.43 percentage points. Compared to traditional PID electronically controlled sowing, the IHBA-LADRC system also showed improvements: the overall qualified index increased by 1.32 percentage points, the reseeding index decreased by 0.49 percentage points, the missed sowing index decreased by 0.76 percentage points, the overall coefficient of variation decreased by 6.30 percentage points, and the variation coefficient of qualified plant spacing decreased by 5.43 percentage points. The IHBA-LADRC-based control system for the electric red bean precision seeder ensures that the actual plant spacing closely matches the theoretical set value. This high level of operational accuracy provides a foundation for implementing precise intercropping between different rows in future applications, thereby further improving land utilization efficiency.

ACKNOWLEDGEMENT

This study was supported by the Key Research and Development Plan Project of Heilongjiang Province (2022ZX05B02), the Heilongjiang Provincial Natural Science Foundation Joint Guidance Project (LH2024E103), and the Heilongjiang Bayi Agricultural University Graduate Innovative Research Project (YJSCX2024-Z02、YJSCX2024-Y12、YJSCX2024-Y13).

REFERENCES

[1] Anandhakumar, C., Murugan, N. S. S., & Kumaresan, K. (2024). Extreme learning machine model with honey badger algorithm based state-of-charge estimation of lithium-ion battery. *Expert Systems with Applications*, 238, 121609. https://doi.org/10.1016/j.eswa.2023.121609

[2] Cay, A., Kocabiyik, H., & May, S. (2018). Development of an electro-mechanic control system for seed-metering unit of single seed corn planters part i: Design and laboratory simulation. *Computers and Electronics in Agriculture*, 144, 71–79. https://doi.org/10.1016/j.compag.2017.11.035

[3] Cay, A., Kocabiyik, H., & May, S. (2018). Development of an electro-mechanic control system for seed-metering unit of single seed corn planters part ii: Field performance. *Computers and Electronics in Agriculture*, 145, 11–17. https://doi.org/10.1016/j.compag.2017.12.021

[4] Chen, J., Zhang, H., Pan, F., Du, M., & Ji, C. (2022). Control system of a motor-driven precision no-tillage maize planter based on the CANopen protocol. *Agriculture*, 12(7), 932. https://doi.org/10.3390/agriculture12070932

[5] Chen, X. (2008). *Automatic disturbance rejection controller parameter tuning method and its application in thermal process* [PhD thesis]. Tsinghua University.

[6] Ding, Y., Li, Y., Zhang, D., Cui, T., Li, Y., Zhong, X., Xie, C., & Ding, Z. (2021). Novel low-cost control system for large high-speed corn precision planters. *International Journal of Agricultural and Biological Engineering*, 14(2), 151-158. https://doi.org/10.25165/j.ijabe.20211402.6053

[7] Gao, Z. (2003). Scaling and bandwidth-parameterization based controller tuning. In *Proceedings of the American Control Conference* (Vol. 6, pp. 4989–4996). Denver, CO, USA.

[8] Hashim, F. A., Houssein, E. H., Hussain, K., Mabrouk, M. S., & Atabany, W. (2021). Honey badger algorithm: New metaheuristic algorithm for solving optimization problems. *Mathematics and Computers in Simulation*, 192, 84-110. https://doi.org/10.1016/j.matcom.2021.08.013

[9] Jafari, M., Hemmat, A., & Sadeghi, M. (2010). Development and performance assessment of a dc electric variable-rate controller for use on grain drills. *Computers and Electronics in Agriculture*, 73(1), 56–65. https://doi.org/10.1016/j.compag.2010.04.004

[10] Kamgar, S., Eslami, M. J., & Maharlouie, M. M. (2013). Design, development and evaluation of a mechatronic transmission system to improve the performance of a conventional row crop planter. Dallas, Texas, July 29-august.2012. https://doi.org/10.13031/2013.41987

[11] Li, Y., Zhou, W., Ma, C., Feng, Z., Wang, J., Yi, S., & Song, W. (2024). Design and optimization of the seed conveying system for belt-type high-speed corn seed guiding device. *International Journal of Agricultural & Biological Engineering*, 17(2), 123-131. https://doi.org/10.25165/j.ijabe.20241702.8427

[12] Ma, C., Yi, S., Tao, G., Li, Y., Wang, S., Wang, G., & Gao, F. (2023). Research on receiving seeds performance of belt-type high-speed corn seed guiding device based on discrete element method. *Agriculture*, 13(5), 1085. https://doi.org/10.3390/agriculture13051085

[13] Ma, J., Khan, N., Gong, J., Hao, X., Cheng, X., Chen, X., Chang, J., & Zhang, H. (2022). From an introduced pulse variety to the principal local agricultural industry: A case study of red kidney beans in Kelan, China. *Agronomy*, 12(7), 1717. https://doi.org/10.3390/agronomy12071717

[14] Mangus, D. L., Sharda, A., Flippo, D., Strasser, R., & Griffin, T. (2017). Development of high-speed camera hardware and software package to evaluate real-time electric seed meter accuracy of a variable rate planter. *Computers and Electronics in Agriculture*, 142, 314–325. https://doi.org/10.1016/j.compag.2017.09.014

[15] Ozumcan, S., Ozturk, A., Vuran, M., & Andic, C. (2023). A novel honey badger algorithm based load frequency controller design of a two-area system with renewable energy sources. *Energy Reports*, 9(12), 272-279. https://doi.org/10.1016/j.egyr.2023.10.002

[16] Priyadarshi, A., Yadav, K., & Rathore, V. (2023). Synchrophasor assisted load frequency control of interconnected system with multiple fuel inputs using honey badger algorithm. *Int. J. Model. Identif. Control*, 43, 54–63. https://doi.org/10.1504/IJMIC.2023.132109

[17] Ranta, O., Drocas, I., Stanila, S., Molnar, A., Muntean, M., Marian, O. (2012). The main advantages of E-drive system used for precision seeding. *Bulletin of the University of Agricultural Sciences and Veterinary Medicine Cluj-Napoca. Agriculture*, 69(1). https://doi.org/10.15835/buasvmcn-agr:8685

[18] Sun, W., Yi, S., Qi, H., Li, Y., Dai, Z., Zhang, Y., & Wang, S. (2024). Design and experiment of progressive seed-cleaning mechanism for air-pressure maize precision seed-metering device. *INMATEH - Agricultural Engineering*, 73, 473-486. https://doi.org/10.35633/inmateh-73-40

[19] Wang, S., Zhao, B., Yi, S., Zhou, Z., & Zhao X. (2022). GAPSO-optimized fuzzy PID controller for electric-driven seeding. *Sensors*, 22(17), 6678. https://doi.org/10.3390/s22176678

[20] Wang, S., Yi, S., Zhao, B., Li, Y., Li, S., Tao, G., Mao, X., & Sun, W. (2024). Sowing depth monitoring system for high-speed precision planters based on multi-sensor data fusion. *Sensors*, 24(19), 6331. https://doi.org/10.3390/s24196331

[21] Wang, S., Yi, S., Zhao, B., Li, Y., Wang, G., Li, S., & Sun, W. (2024). Photoelectric sensor-based belt-type high-speed seed guiding device performance monitoring method and system. *Computers and Electronics in Agriculture*, 227, 109489. https://doi.org/10.1016/j.compag.2024.109489

[22] Xu, T., Fu, H., Yu, J., Li, C., Wang, J., & Zhang, R. (2024). Determination of ellipsoidal seed–soil interaction parameters for DEM simulation. *Agriculture*, 14(3), 376. https://doi.org/10.3390/agriculture14030376

[23] Yi, S., Wang, G., Li, Y., Wang, S., Li, S., & Wei, R. (2025). Design and Experiment of Seed Orientation Correction Element for High-speed Belt-type Soybean Seeding Device. *Transactions of the Chinese Society for Agricultural Machinery*, 56(5), 268–278+424. https://doi.org/10.6041/j.issn.1000-1298.2025.05.025

[24] Yousri, D., Allam, D., Eteiba, M. B. (2019). Chaotic heterogeneous comprehensive learning particle swarm optimizer variants for permanent magnet synchronous motor. *Applied Soft Computing*, 74, 479–503. https://doi.org/10.1016/j.asoc.2018.10.032

[25] Zhang, Y., Sun, W., Yu, H., Geng, X., Fan, M., & Qin, M. (2022). An improved model-free predictive current control method for PMSM drives based on extended control set and fast current difference updating. *IEEE Energy Conversion Congress and Exposition (ECCE)*, Detroit, MI, USA, 2022, 1-8, *https://doi.org/10.1109/ECCE50734.2022.9947757*